Atmospheric Environment 180 (2018) 126–137

Contents lists available at ScienceDirect

Atmospheric Environment

journal homepage: www.elsevier.com/locate/atmosenv

Emission of intermediate, semi and low volatile organic compounds from traffic and their impact on secondary organic aerosol concentrations over Greater Paris

K. Sartelet[a,*], S. Zhu[a,b], S. Moukhtar[c], M. André[d], J.M. André[e], V. Gros[f], O. Favez[g], A. Brasseur[h], M. Redaelli[h]

[a] CEREA, Joint Laboratory Ecole des Ponts ParisTech/EdF R&D, Université Paris-Est, Marne la Vallée, France
[b] Now at Department of Mechanical and Aerospace Engineering, University of California at Irvine, California, USA
[c] Airparif, Paris, France
[d] IFSTTAR, Bron, France
[e] CITEPA, Paris, France
[f] LSCE, Gif-sur-Yvette, France
[g] INERIS, Verneuil-en-Halatte, France
[h] Anses, Maisons-Alfort, France

ARTICLE INFO

Keywords:
Intermediate volatile organic compounds
Secondary organic aerosols
Particles
Emissions
Traffic

ABSTRACT

Exhaust particle emissions are mostly made of black carbon and/or organic compounds, with some of these organic compounds existing in both the gas and particle phases. Although emissions of volatile organic compounds (VOC) are usually measured at the exhaust, emissions in the gas phase of lower volatility compounds (POA_{vapor}) are not. However, these gas-phase emissions may be oxidised after emission and enhance the formation of secondary organic aerosols (SOA). They are shown here to contribute to most of the SOA formation in Central Paris. POA_{vapor} emissions are usually estimated from primary organic aerosol emissions in the particle phase (POA). However, they could also be estimated from VOC emissions for both gasoline and diesel vehicles using previously published measurements from chamber measurements. Estimating POA_{vapor} from VOC emissions and ageing exhaust emissions with a simple model included in the Polyphemus air-quality platform compare well to measurements of SOA formation performed in chamber experiments. Over Greater Paris, POA_{vapor} emissions estimated using POA and VOC emissions are compared using the HEAVEN bottom-up traffic emissions model. The impact on the simulated atmospheric concentrations is then assessed using the Polyphemus/Polair3D chemistry-transport model. Estimating POA_{vapor} emissions from VOC emissions rather than POA emissions lead to lower emissions along motorway axes (between −50% and −70%) and larger emissions in urban areas (up to between +120% and +140% in Central Paris). The impact on total organic aerosol concentrations (gas plus particle) is lower than the impact on emissions: between −8% and 25% along motorway axes and in urban areas respectively. Particle-phase organic concentrations are lower when POA_{vapor} emissions are estimated from VOC than POA emissions, even in Central Paris where the total organic aerosol concentration is higher, because of different assumptions on the emission volatility distribution, stressing the importance of characterizing not only the emission strength, but also the emission volatility distribution.

1. Introduction

Particles, especially fine particles, lead to adverse effects on human health (e.g. Pope et al., 1995), and to visibility reduction. They also affect the manner in which radiation passes through the atmosphere and represent an uncertain component of climate change. Particles are made of different compounds: dust, inorganic aerosol, organic aerosol (OA), black carbon (BC), metals, etc. Organic compounds have a large range of molecular weights and functionalities, which determine their volatility (their capacity to partition between the gas and particle phases), and other properties (e.g. their water solubility, which affects their capacity to partition to the particle phase depending on the environment). Volatile organic compounds (VOC) are usually defined as compounds that only exist in the gas phase (roughly ≤ C_{12}, see Gentner

* Corresponding author.
E-mail address: karine.sartelet@enpc.fr (K. Sartelet).

https://doi.org/10.1016/j.atmosenv.2018.02.031
Received 19 July 2017; Received in revised form 2 January 2018; Accepted 15 February 2018
Available online 05 March 2018
1352-2310/

et al. (2017)). Organic aerosol may exist in both the gas (OA_{vapor}) and particle (OA) phases (Robinson et al., 2007). The total of the gas and particle phases of organic aerosol is referred to as OA_{total}, following the naming convention of Murphy et al. (2014). OA_{total} is made of different compounds, which are usually classified depending on their volatility: intermediate volatility organic compounds (IVOC), semi volatility organic compounds (SVOC) and low volatility organic compounds (LVOC). A glossary summarizing the notation used is provided in Appendix A.

Atmospheric concentrations. In the atmosphere, high concentrations of OA are observed in winter in some urban areas (Petit et al., 2015; Cheng et al., 2016). In summer, OA concentrations may mostly originate from the oxidation of biogenic VOC emitted from the vegetation (Sartelet et al., 2012; Chrit et al., 2017). However, in winter in urban areas, OA concentrations may mostly originate from the oxidation of anthropogenic VOC and gas-phase organic aerosol of volatility lower than VOC (OA_{vapor}). These VOC and OA_{vapor} may have different origins, such as wood-burning and traffic-related activities (Baudic et al., 2016; Denier van der Gon et al., 2015; Beekmann et al., 2015). Air-quality models, which simulate the fate of organic compounds in the atmosphere, tend to under-estimate OA concentrations in urban areas (Couvidat et al., 2013; Hayes et al., 2015). This under-estimation could be partly due to the gas-phase primary organic aerosol emissions (POA_{vapor}), which are currently missing from most emission inventories (Robinson et al., 2007; Couvidat et al., 2012; Denier van der Gon et al., 2015).

Organic precursors from traffic. For a long time, it was assumed that vehicular-derived particles were predominantly a direct tailpipe emission, but recent studies indicate that a larger fraction is secondary (Platt et al., 2013; Gordon et al., 2014a, b), i.e. it is formed through atmospheric physico-chemical processes of precursors, which form secondary organic aerosols (SOA, Zhang et al., 2007; Jimenez et al., 2009). Organic compounds emitted from gasoline and diesel vehicles are found in both the gas and particle phases (Schauer et al., 1999, 2002). Exhaust (primary emitted) particles were considerably reduced by the introduction of particle filters in diesel vehicles (DPF) (Platt et al., 2013; Gordon et al., 2014b; Kim et al., 2016). Platt et al. (2013) and Gordon et al. (2014a, b) measured directly the ageing of the exhaust emissions in reaction chambers from tested vehicles incorporating a range of engines and exhaust aftertreatment technologies, including DPF and diesel oxidation catalysts. They found that the SOA fraction, formed from the oxidation of VOC and POA_{vapor}, largely dominates the primary organic aerosol (POA) fraction (e.g. Gentner et al., 2017). Amongst VOC, the main known precursors are aromatics (Odum et al., 1997; Dawson et al., 2016), such as the so-called BTEX (benzene, toluene, ethylbenzene, and xylene). Although gasoline fuel contains a larger percentage of aromatics than diesel fuel (Louis et al., 2016), Martinet et al. (2017) measured similar BTEX emissions from recent gasoline and diesel vehicles. However, Euro 1 and Euro 2 gasoline vehicles emit 10 times more BTEX than recent vehicles. Gas and particle phase primary organic aerosol (POA_{total}) are made of different chemical species, such as high molecular weight alkanes ($> C_{12}$), high molecular weight aromatics and cyclic compounds, which are likely to be the major contributors to SOA (Schauer et al., 1999, 2002; May et al., 2014; Zhao et al., 2015, 2016).

POA_{total} emissions. Air-quality models, such as the one of the air-quality modelling platform Polyphemus used here, use emission inventories as input data to compute the concentrations of pollutants. Although VOC emissions are provided by emission inventories, POA_{vapor} emissions are not. Because of their semi-volatile properties, measurements of POA_{total} in the exhaust are difficult. For example, POA_{total} may condense on or evaporate from filters depending on the dilution and atmospheric conditions, e.g., temperature, leading to uncertainties in measuring organic particles. Furthermore, the gas/particle emission ratio (POA_{vapor}/POA) depends on the time elapsed between emissions and measurements. Kim et al. (2016) estimated that depending on vehicles and road-driving cycles, thermodynamic equilibrium between gas and particles may take up to 8 min to be reached. A time elapsed between emission and measurement shorter than this characteristic time to reach equilibrium can lead to lower concentrations in the particle phase than those that would be estimated assuming thermodynamic equilibrium, because the equilibrium between gas and particles has not yet been reached. Therefore, measurements of OA performed using online (e.g. aerosol mass spectrometers) and off-line (e.g. filters) measurement techniques may lead to different gas/particle ratio POA_{vapor}/POA. Because of the difficulties to estimate POA_{total} emissions, they have been estimated using different methods, such as measurements performed for linear alkanes (Kim et al., 2016). Kim et al. (2016) estimated that the gas/particle ratio of alkane emissions for passenger cars in France is about 1.5. By assuming that the gas/particle ratio of emissions is the same as the ratio of alkane emissions, Zhu et al. (2016) used this 1.5 ratio to compute winter air-quality over Greater Paris, and found relatively good agreement with measurement for January 2009. Other publications used the same POA_{vapor}/POA ratio of 1.5 to estimate POA_{total} (Bergström et al., 2012; Koo et al., 2014).

Because measurements of POA depend on temperature, Jathar et al. (2014b) and Zhao et al. (2015, 2016) recommend to estimate emissions of POA_{vapor} using a IVOC/NMHC ratio, with NMHC being non-methane hydrocarbons. Following the measurements of May et al. (2013a, b) and Gordon et al. (2014a, b), and by performing a gas-phase carbon-balance analysis, Jathar et al. (2014b) determines the average contribution of unspeciated organic compounds (assumed to be mainly IVOCs) to non-methane organic gas (NMOG). Zhao et al. (2015, 2016) quantified IVOC emissions for a fleet of gasoline and diesel vehicles through gas chromatography/mass spectrometry analysis of adsorbent samples collected from a constant volume sampler. Zhao et al. (2016) found a IVOC/NMHC ratio similar to Jathar et al. (2014b) for gasoline vehicles (a ratio IVOC/NMHC of about 17% against a ratio IVOC/NMOG of 25% in Jathar et al. (2014b)), but lower for diesel vehicles (a ratio IVOC/NMHC of about 60% against a ratio IVOC/NMHC of 20% in Jathar et al. (2014b)). Note that the difference between NMOG and NMHC, which is of the order of 10% (Gierczak et al., 2017), may not explain the differences between the two approaches for diesel vehicles, for which a large fraction of IVOC may not be accounted for in NMHC measurements (Zhao et al., 2016).

Jathar et al. (2014a) and Zhao et al. (2015, 2016) modelled in 0D the ageing of exhaust emissions by taking into account the molecular structure of IVOC. Jathar et al. (2014a) showed that SOA formation may be sufficiently well reproduced in air-quality model by modelling the ageing of IVOC precursors as a fuction of the precursor volatility, without differences in the molecular structure.

IVOC emissions have often been included in air-quality models, proportionally to POA emissions, resulting in better model to measurements comparisons in terms of both SOA magnitude and diurnal variability (e.g. Dzepina et al., 2009; Hodzic et al., 2010; Couvidat et al., 2013; Hayes et al., 2015; Woody et al., 2016; Murphy et al., 2017). Jathar et al. (2017) used the ratio estimated by Jathar et al. (2014b) in the air-quality model CMAQ to estimate IVOC emissions by reapportioning the existing NMOG emissions between VOC and IVOC. They found that over southern California, IVOC forms as much SOA as VOC, in agreement with chamber experiments performed using emissions of gasoline vehicles (Gordon et al., 2014b; Zhao et al., 2016). The contribution of IVOC to air quality may be even more important in Europe, where diesel vehicles are more common than in North America (Dunmore et al., 2015). Ots et al. (2016) presented a first estimation of diesel IVOC emissions for European cities. They estimated IVOC emissions to be about 2.3 times the amount of VOC emissions from diesel and gasoline vehicles. Their estimation is higher than those of Gordon et al. (2014a) and Zhao et al. (2015). Their IVOC emissions were estimated from the measured ratio of diesel IVOC + VOC concentrations to gasoline-VOC concentrations measured in Central London during the

ClearfLo campaign.

This work presents a new emission model built on the measurements of Zhao et al. (2015, 2016) to estimate POA_{total} (IVOC, SVOC and LVOC) emissions from VOC emissions. These emissions are added to vehicular VOC and NO_x emissions, and the SOA formation from ageing of those emissions as modelled with the air-quality platform Polyphemus is compared to the chamber experiments of Platt et al. (2013); Gordon et al. (2014a, b) and to the model of Zhao et al. (2015, 2016). The air-quality model of Polyphemus is then used for 3D-simulation over Greater Paris. POA_{total} emissions computed from the POA_{total}/VOC emission ratio are compared to those computed from the POA_{total}/POA emission ratio, and the impact on OA concentrations is estimated, as well as the influence of the emission volatility.

2. Emissions

2.1. Estimation of the primary emissions

POA_{total} is divided into three different classes of volatility: POA-iv (intermediate volatility), POA-sv (semi volatility) and POA-lv (low volatility).

Emissions of POA-iv are estimated from the POA-iv/NMHC emission ratio quantified by Zhao et al. (2015, 2016) through gas chromatography/mass spectrometry analysis of adsorbent samples collected from a constant volume sampler. Zhao et al. (2015) recommend using POA-iv/NMHC = 0.6 ± 0.1 for diesel vehicles without DPF and POA-iv/NMHC = 1.5 ± 0.8 for diesel vehicles with DPF. Zhao et al. (2016) recommend using POA-iv/NMHC = 0.04 ± 0.02 for cold-start gasoline vehicles and 0.17 ± 0.12 for hot-start gasoline vehicles. Although NMHC is defined as the total of non-methane hydrocarbons, Zhao et al. (2015, 2016) showed that NMHC does not include all POA_{vapor} and that it is difficult to estimate the part of POA_{vapor} included in the measured NMHC. Zhao et al. (2015) suggested that about 2/3 of POA-iv are not taken into account in NMHC measurements for diesel vehicles with DPF. In this work, given the significant uncertainties in determining the POA-iv/NMHC emission ratio and the POA-iv fraction included in the measured NMHC value, the POA-iv/VOC emission ratio is assumed to be equal to the POA-iv/NMHC ratio, and VOC emissions are therefore used to calculate those of POA-iv. This approximation is correct for gasoline vehicles for which POA-iv emissions are low relative to VOC emissions and for diesel vehicles without DPF. Indeed, assuming that 2/3 of the POA-iv are included in the NMHC, for diesel vehicles without DPF, the POA-iv/VOC emission ratio is equal to 0.68, i.e. it is very close to the POA-iv/NMHC emission ratio of 0.6 ± 0.1; for gasoline vehicles, the POA-iv/VOC emission ratio is exactly equal to the POA-iv/NMHC emission ratio to the nearest two decimal digits (POA-iv/VOC = 0.04 for cold-start gasoline vehicles and POA-iv/VOC = 0.17 for hot-start gasoline vehicles). However, this methodology could underestimate the POA-iv of diesel vehicles without DPF for which POA-iv/NMHC = 1.5 ± 0.8 and POA-iv/VOC = 6 if 2/3 of the POA-iv are not taken into account in the NMHC measurements. However, since the volatility of POA-iv emissions from diesel vehicles without and with DPF are different (Zhao et al., 2015), it is likely that the POA-iv fraction in NMHC recommended for diesel vehicles without DPF is not correct for diesel vehicles with DPF, and the ratio POA-iv/VOC is therefore highly uncertain for diesel vehicles with DPF.

POA-sv and POA-lv emissions are estimated from POA-iv emissions using the volatility class distributions of POA_{total} emissions determined by Zhao et al. (2015, 2016). Nine volatility classes are defined in Zhao et al. (2015, 2016). Emissions of the most volatile class are not considered, they are assumed to be too volatile to form organic aerosols effectively. Furthermore, part of those emissions might be included in VOC emissions. The eight remaining volatility classes are aggregated into three classes of volatility (low, medium and high), corresponding to the species used in Polyphemus (POA-lv, POA-sv and POA-iv respectively), as detailed in Tables B.4, B.5 and B.6. Note that for diesel vehicles with DPF, Zhao et al. (2015) do not specify the mass fraction of the lowest volatility class. It is estimated such that the sum of the mass fractions equals 1, as for diesel vehicles without DPF. Using the assumptions detailed above, the relations to compute POA-lv, POA-sv and POA-iv emissions from VOC emissions are detailed in Appendix C.

2.2. Ageing of emissions

After emission into the atmosphere, the oxidation of VOC and POA_{vapor} leads to less volatile compounds than the precursors. These compounds condense more easily onto particles than their precursors and they contribute to the increase of particle mass. In this work, ageing of POA_{vapor} is performed following Couvidat et al. (2012):

$$POA_{vapor}\text{-lv} + OH \rightarrow SOA_{vapor}\text{-lv} \quad (1)$$

$$POA_{vapor}\text{-sv} + OH \rightarrow SOA_{vapor}\text{-sv} \quad (2)$$

$$POA_{vapor}\text{-iv} + OH \rightarrow SOA_{vapor}\text{-iv} \quad (3)$$

where POA_{vapor}-lv, POA_{vapor}-sv and POA_{vapor}-iv are characterized by their saturation concentrations C^*: $\log(C^*) = -0.04$, 1.93 and 3.5; SOA-lv, SOA-sv and SOA-iv are surrogates representing aged POA-lv, POA-sv and POA-iv ($\log(C^*) = -2.4$, -0.064 and 1.5 respectively). The partitioning between the gas and particle organic phases is modelled with the SOAP numerical model (Couvidat and Sartelet, 2015).

To estimate how this simple ageing model performed compared to the more detailed model of Zhao et al. (2015, 2016) and to the measurements performed by Gordon et al. (2014a, b) and Platt et al. (2013), VOC emission factors are distributed according to specific molecular species, using the VOC speciation recommended by Theloke and Friedrich (2007). The gaseous chemistry and the oxidation of VOC are modelled with the CB05 chemical mechanism modified to represent the formation of SOA from toluene and xylene (Kim et al., 2011). The POA_{total} emissions are estimated as detailed in the previous section and in Appendix C.

For the comparisons to Zhao et al. (2015, 2016) and Gordon et al. (2014a, b), for the different vehicle types, the NO_x concentrations are initialized, such as being typical of urban environment (high NO_x regime): the ratio VOC/NO_x in ppbC ppb NO_x^{-1} is taken equal to 3, as in the experiments of Gordon et al. (2014a, b). NO_x are speciated as 100% NO. The model of Zhao et al. (2015, 2016) uses high-NO_x yields for SOA formation with a constant OH concentration, assumed to be equal to $1.5 \times 10^6\ cm^{-3}$.

For diesel vehicles without DPF and idle driving, the averaged VOC emission factor (EF) from Zhao et al. (2015) is about EF VOC = 6 200 mg/kg fuel. This factor is scaled to have the formation of particulate organic compounds of about $10\ \mu g\ m^{-3}$ at the end of the simulation, as advocated by Zhao et al. (2015). After 48 h of ageing, our model simulates the formation of $8.2\ \mu g\ m^{-3}$ of SOA, i.e. 1 574 mg/kg fuel. This value is very close to that obtained by Zhao et al. (2015): 1 500 mg/kg fuel with a standard deviation of about 500 mg/kg fuel. After 11 h of ageing, the OH exposure time is similar to the exposure time of the experiments of Gordon et al. (2014b) (assuming a constant OH concentration of $10^7\ cm^{-3}$ in the experiment), and the ratio SOA/POA is equal to 6.6, which agrees relatively well to the ratio 8.6 measured in Gordon et al. (2014b). This ratio is not very sensitive to the NO_x and propene concentrations because most of SOA is formed from the oxidation of POA_{vapor} (left panel of Fig. 1), which assumes that the oxidation does not depend on NO_x levels.

For diesel vehicles without DPF, and high-speed driving, the averaged VOC emission factor from Zhao et al. (2015) is about EF VOC = 1 300 mg/kg fuel. This factor is scaled to have the formation of particulate organic compounds of about $10\ \mu g\ m^{-3}$ at the end of the simulation, as advocated by Zhao et al. (2015). After 48 h of ageing, our model simulates the formation of $10.0\ \mu g\ m^{-3}$ of SOA, i.e. 360 mg/kg fuel. This value is within the range of what was obtained by Zhao et al.

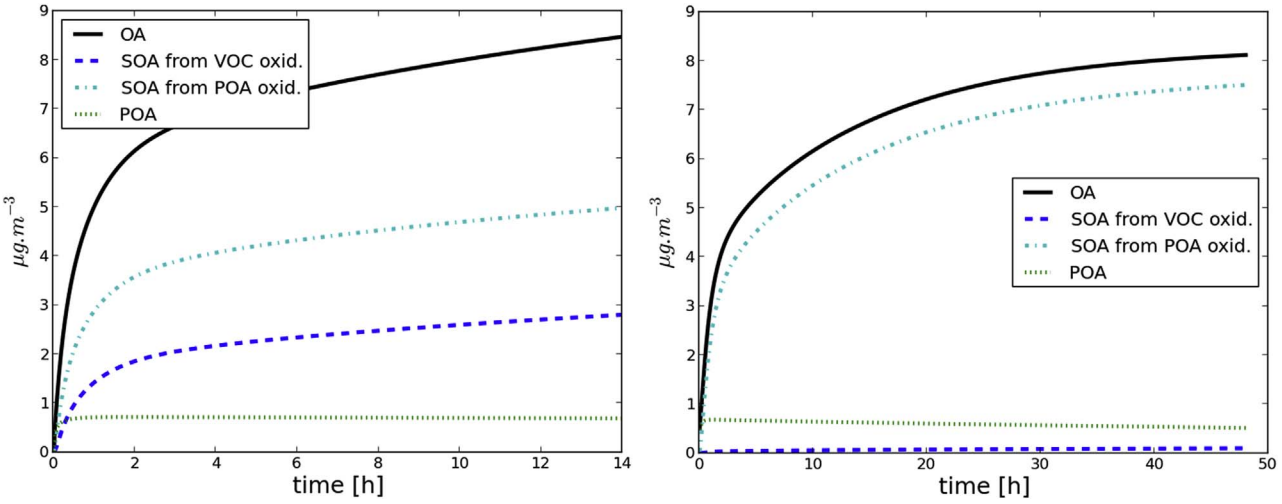

Fig. 1. SOA formation for idle driving diesel vehicle without DPF (left panel) and for cold-start gasoline vehicle (right panel). The temporal evolution of OA concentrations is plotted with a black solid line. OA concentrations are the sum of POA concentrations (green dotted line), SOA concentrations originating from VOC oxidation (dark blue dashed line) and SOA concentrations originating from POA_{vapor} oxidation (light blue dotdashed line line). (For interpretation of the references to colour in this figure legend, the reader is referred to the Web version of this article.)

(2015): 250 mg/kg fuel with a standard deviation of about 150 mg/kg fuel. As for diesel vehicles without DPF and idle driving, most SOA are formed from oxidation of POA_{vapor}. After 11 h of ageing, the OH exposure time is similar to the exposure time of the experiments of Gordon et al. (2014b) (assuming a constant OH concentration of $10^7\,cm^{-3}$ in the experiment), and the ratio SOA/POA is equal to 2.8, which agrees relatively well to the ratio 2.3 measured in Gordon et al. (2014b).

For cold-start gasoline vehicles, the averaged VOC emission factor from Zhao et al. (2016) is about EF VOC = 1 500 mg/kg fuel. This factor is scaled to have the formation of particulate organic compounds of about $10\,\mu g\,m^{-3}$ at the end of the simulation, which is run for 14 h to have a similar OH exposure time as Zhao et al. (2016) (after 14 h of simulation, OH concentrations here are lower than the constant OH concentrations of Zhao et al. (2016)). As advocated by Zhao et al. (2016), we assume that POA-iv = 0.04 VOC. After 14 h of ageing, the formation of SOA is $8.4\,\mu g\,m^{-3}$, i.e. 33.6 mg/kg fuel. Zhao et al. (2016) estimated an SOA/POA emission ratio of about 2.6 after 14 h of photochemical oxidation. Zhao et al. (2016) showed that POA are linked to POA-iv by the relationship POA-iv/POA = 6.2 ± 4.4. We can therefore estimate the POA to be about POA = POA-iv/6.2 = 9.7 mg/kg fuel. The SOA/POA ratio is thus 33.6/9.7 = 3.4 for the simulation, which is close to the value of 2.6 obtained by Zhao et al. (2016). The right panel of Fig. 1 shows that about two third of SOA are formed from POA_{vapor} oxidation. The SOA/POA ratio after 14 h of simulation is 3.4, which is lower than the ratio observed in Gordon et al. (2014a), which ranges between 8 and 15. This difference may be due to differences in OH concentrations and in the chemical regimes. In Gordon et al. (2014a), the average OH concentration is $5 \times 10^6\,cm^{-3}$, which is more than 3 times higher than here. In Gordon et al. (2014a), OH concentrations are obtained by the photolysis of HONO, which also forms NO, and propene was added to the chamber to reach a VOC/NO_x ratio of 3. In our simulation, by artificially adding propene and NO (about 400 ppb) at the initial time of the simulation and by choosing propene concentration, such as having a ratio VOC/NO_x of about 3, the simulation forms higher SOA concentrations than the simulation where propene and NO are not added. The SOA/POA ratio is about 4.3 after 3 h (same OH exposure time as Gordon et al. (2014a)), against a SOA/POA ratio of 3.0 without propene but same OH exposure time. These differences are due to the influence of NO concentration on the formation of SOA from the oxidation of VOC (NO_x dependent). The remaining discrepancy between model and measurements may be due to missing SOA precursors as suggested by Gentner et al. (2017), or by uncertainties in the POA measurements as suggested by Zhao et al. (2016), which are relatively low and very sensitive to temperature and organic concentrations, and uncertainties in the volatility of OA.

Platt et al. (2013) performed ageing experiments on a recent Euro 5 gasoline car. They monitored the total hydrocarbon mass (THC) as well as OA concentrations. In our model, THC is obtained as the sum of POA_{total} and VOC, and it is initialized as measured in the experiments of Platt et al. (2013) before lights-on (1.4 ppmv + 0.9 ppmv of propene). POA_{total} is estimated from VOC emissions using the ratio 0.17 estimated by Zhao et al. (2016), and NO_x concentrations are initialized such as having a VOC/NO_x ratio equal to 5.6 as in Platt et al. (2013). After 5 h of ageing, $197\,\mu g\,m^{-3}$ of OA are simulated in good agreement with the measurements of Platt et al. (2013), who estimated OA to be about $200\,\mu g\,m^{-3}$ after wall loss corrections. As estimated by Platt et al. (2013), the contribution of VOC precursors to OA is low (about 17%). The better agreement between the model and the measurements of Platt et al. (2013) than those of Gordon et al. (2014a) may be due to uncertainties in the partitioning of OA, which partitions probably more in the particle phase in the experiments performed by Platt et al. (2013) as OA concentration is higher. Furthermore, we assumed the POA_{total}/VOC ratio to be equal to 0.17 for the experiment of Platt et al. (2013), whereas we took a lower "cold-start" ratio (0.04) for the experiment of Gordon et al. (2014a).

3. Application to Greater Paris (Île-de-France region)

3.1. Model presentation

The simulations are carried out with the eulerian model Polair3D of the Polyphemus air quality modelling platform. The model set-up is the same as described in Zhu et al. (2016).

In order to simulate pollutant concentrations over Greater Paris (Île-de-France region), nested simulations (domains Europe, France and Île-de-France) are carried out (Fig. 2). Concentrations over Europe are simulated for the year 2014 (from 1 January to 31 December). These concentrations served as initial and boundary conditions for simulations over France (from 4 January to 31 December), which themselves served as initial and boundary conditions for simulations over Île-de-France (from 8 January to 31 December). The initial and boundary conditions of the Europe simulation are obtained from the MOZART-4 global model and the meteorological fields of the NASA GMAO GEOS-5

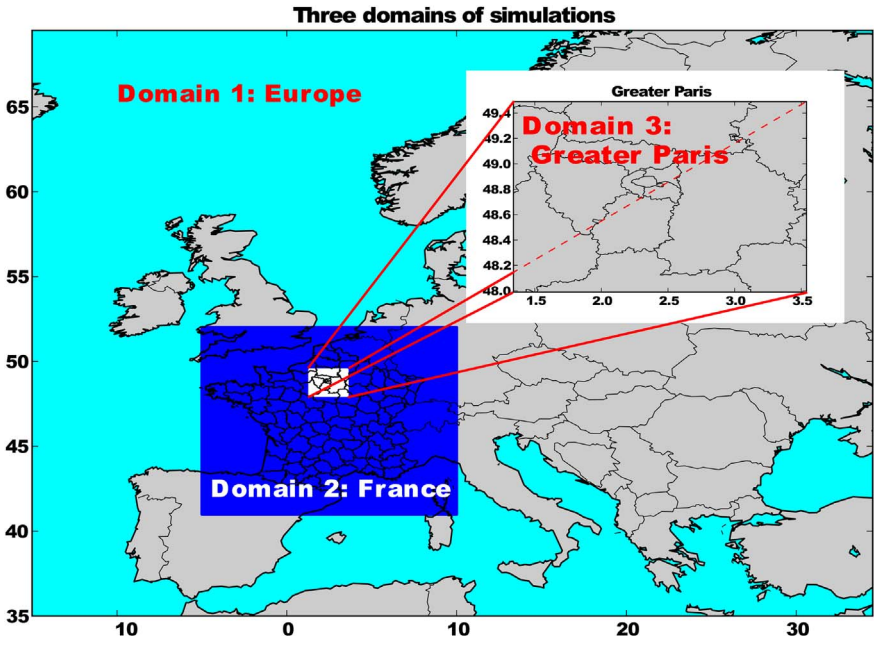

Fig. 2. Nested simulation domains.

model (http://www.acom.ucar.edu/wrf-chem/mozart.shtml, Emmons et al., 2010). For the Europe and France simulations, the European Center for Medium-Range Weather Forecasts (ECMWF) reanalysis meteorological fields are interpolated on the grids of Polyphemus. For the Île-de-France simulation, meteorology is simulated with the Weather Research and Forecasting (WRF) model 3.6 (Skamarock et al., 2008), and the Corine land-use database (Kim et al., 2013).

Emissions of marine salts are estimated using the parametrisation of Jaeglé et al. (2011). Biogenic emissions are estimated using the MEGAN model (Model of Emissions of Gases and Aerosols from Nature, Guenther et al., 2006). Over Europe, anthropogenic emissions for gases and particulates are obtained from the EMEP emission inventory (Vestreng, 2003), while they are obtained from CITEPA over France. For traffic, VOC emissions are specified according to Theloke and Friedrich (2007), which allow the speciation to depend on the engine type (diesel, gasoline). The NO_x speciation is calculated according to the distribution of the vehicle fleet following the EMEP guide (Ntziachristos et al., 2008), which leads to about 73.2% of NO, 26% of NO_2 and 0.8% of HONO over France. For particles, the speciation is also defined according to vehicle types, using the EMEP guide BC/$PM_{2.5}$ and OA/BC ratios (Ntziachristos et al., 2008). Accordingly, particles are speciated into about 60.9% of BC, 19.9% of OA and 19.2% of dust. Although the exhaust emits only BC and OA, some of the emissions are specified as dust because the emission factors used for $PM_{2.5}$ for the traffic sector in the EMEP inventory partially account for resuspension. Over Île-de-France, emissions were provided by Airparif (www.airparif.fr), using the HEAVEN bottom-up traffic emissions model (http://www.transport-research.info/sites/default/files/project/documents/20090917_162316_73833_HEAVEN-FinalReport.pdf). They are specified for the different engine technologies. The fleet and technology data required for the calculation of emissions are obtained from the city of Paris (data for 2014), from data specific to Île-de-France for areas outside Paris (data collected during the ZaParc project, 2013), and from data transmitted by the STIF for the urban bus fleet. On average, about 66% of passenger cars are assumed to be diesel, 31% are gasoline and 3% are hybrid or electric vehicles, while almost all of medium and heavy duty vehicles are diesel. The Parisian fleet is also characterized by an important share of two-wheelers motorized vehicles: while national data report only 4% on average in urban areas (https://www.citepa.org/fr/activites/inventaires-des-emissions/secten#Contribution_ss-secteurs), the stock of this type of vehicles reaches an average of 21% at the morning rush hour. Similarly to the France simulation, the VOC speciation is computed from Theloke and Friedrich (2007) and the NO_x and particle speciation from Ntziachristos et al. (2008).

3.2. POA_{total} emissions and volatility distribution

On average over Greater Paris, POA_{total} emissions estimated from the POA_{total}/POA emission ratio and the POA_{total}/VOC emission ratios are similar (2 357 tonnes per year using the POA_{total}/POA ratio, and 2 402 tonnes per year using the POA_{total}/VOC ratios). However, strong spatial variations exist. Fig. 3 shows the POA_{total} emissions estimated from the POA_{total}/POA ratio and the relative differences between the POA_{total} emissions estimated from the POA_{total}/VOC ratios and those estimated from the POA_{total}/POA emission ratio. When emissions are calculated from the POA_{total}/VOC ratios, POA_{total} emissions are much higher in urban areas (between +120% and +140% in Central Paris and between 30% and 120% in urban areas), while they are lower along motorway axes (between −50% and −70%). These differences are due to spatial differences in POA and VOC emissions, as shown in Fig. 4. VOC emissions are higher in urban areas than along motorway axes, which is not the case for POA emissions. It is also important to note that a large disparity exists in the volatility repartition of POA_{total} emissions depending on the model used. In Couvidat et al. (2012), 25%, 32% and 43% of POA_{total} emissions are distributed into POA-lv, POA-sv and POA-iv classes respectively. However, using the parameterisations presented in this paper, POA_{total} emissions are more volatile: 5.9%, 9.7% and 84.4% are distributed into POA-lv, POA-sv and POA-iv classes respectively (Appendix B). Uncertainties in the volatility distribution is high: although the volatility distribution used in the new parameterisation presented here is based on the measurements of May et al. (2013a, b), Kuwayama et al. (2015) suggest that it may be too volatile and that a large fraction of POA_{total} may actually be nonvolatile, i.e. closer to the volatility distribution used in our reference simulation.

3.3. Model evaluation

For evaluation, the model is compared to concentrations measured at background Airparif stations for O_3, NO_2, PM_{10}, $PM_{2.5}$ and BC, as well as to OA measured at the background sub-urban site SIRTA (Site

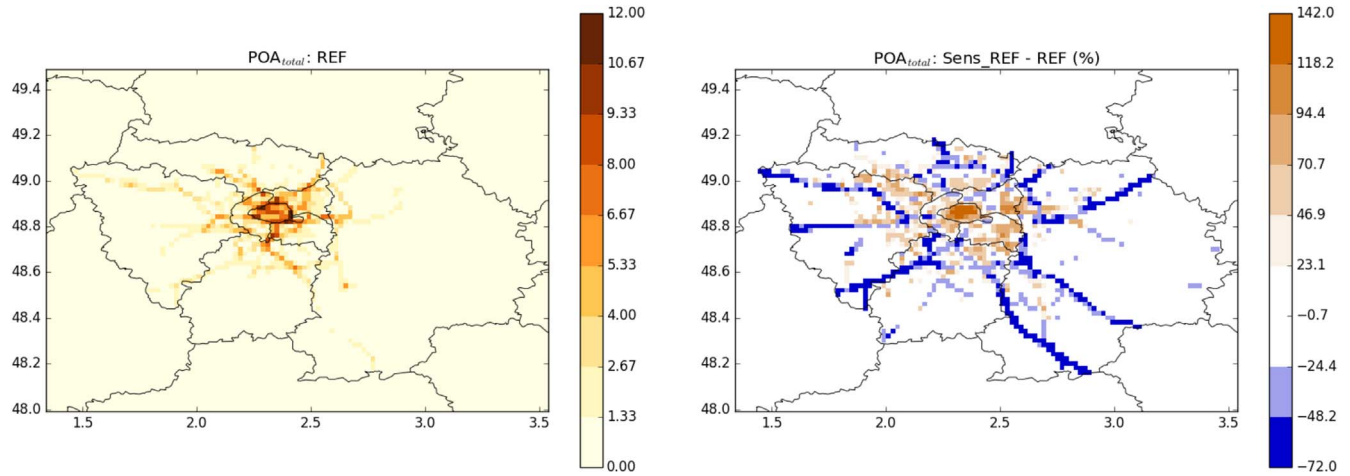

Fig. 3. POA_{total} emissions due to traffic in tonnes per year estimated from emissions of POA (reference simulation, left panel), and relative difference between the POA_{total} emissions estimated from the emissions of VOC (sensitivity study) and the emissions of POA (reference) (right panel).

Instrumental de Recherche par Télédétection Atmosphérique, see Fig. 5 for the location of the stations). To evaluate the simulations with respect to the observations, different statistics are calculated including the meanand the correlation coefficient between the observations and the simulation. For O_3, the mnge (mean normalised gross error) and the mngb (mean normalised gross bias) are also calculated with a usual cut-off threshold of 80 $\mu g\,m^{-3}$. Russell and Dennis (2000) recommend as a performance criterion for hourly concentrations of O_3: $|mngb| \leq 15\%$ and $mnge \leq 30\%$. For particulate matter, the mfe (mean fractional error) and the mfb (mean fractional bias) are calculated. Boylan and Russell (2006) recommend as a goal criterion for the daily concentrations: $mfe \leq 50\%$ and $|mfb| \leq 30\%$, and as a performance criterion: $mfe \leq 75\%$ and $|mfb| \leq 60\%$.

Table 1 and Table 2 show the statistics obtained for O_3, NO_2, PM_{10}, $PM_{2.5}$, BC and OA. Although the mean concentration of ozone is overestimated, the simulation largely satisfies the criterion of Russell and Dennis (2000), which focuses on high concentrations of ozone.

Concerning NO_2, the simulation underestimates the observations. There are no established criteria for comparisons of simulated and observed NO_2 concentrations. However, the statistics obtained are comparable to those obtained in other studies and/or other models (Roustan et al., 2011; Zhang et al., 2013; Terrenoire et al., 2015). Because NO_2 is primarily emitted from surface-based sources, model performance could be improved with a finer spatial resolution and using more realistic emission factors (Ntziachristos et al., 2016). For particulate matter, mean PM_{10} concentrations tend to be underestimated, while $PM_{2.5}$ concentrations are slightly overestimated. However, the performance criterion and even the goal criterion are met. For BC, the simulation under-estimates the mean concentrations, but the errors meet the performance goal criterion and the correlation is high (56%). For OA, the performance and goal criteria are verified.

3.4. Impact of the emission model on the concentrations

POA_{total} emissions influence the concentrations of organic aerosol in the particle phase (OA). In the simulation, the contribution of POA_{total} emissions to OA concentrations is as high as 20–60%, and it is much higher than the contribution of VOC emissions, which is lower than 5% (Fig. 6).

The differences between the emissions estimated from the POA_{total}/POA emission ratio and the POA_{total}/VOC emission ratios range between −70% and 140%. They are greater than the differences between the concentrations, which range between −22% and 0%. Furthermore, the OA concentrations simulated using POA_{total} emissions computed from the POA_{total}/POA emission ratios (reference simulation) are higher than those simulated using POA_{total} emissions computed from the POA_{total}/VOC emission ratios (sensitivity simulation), especially along motorway axes, where POA_{total} emissions are up to 50%–70% lower in the sensitivity simulation (Fig. 7). This is also true in Central Paris, although POA_{total} emissions are up to two times higher if they are

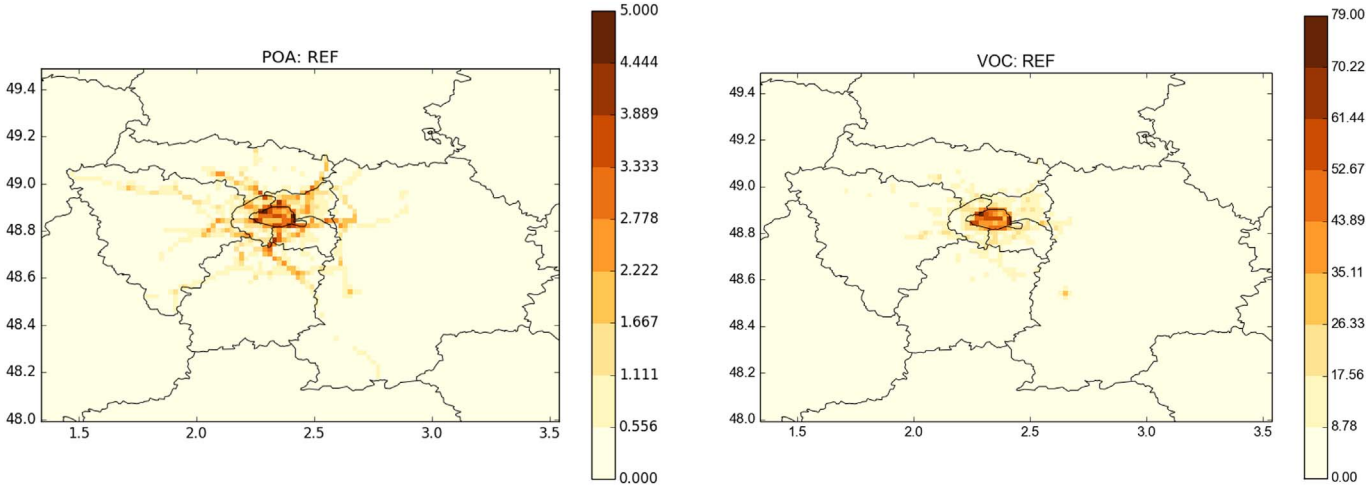

Fig. 4. Emissions due to traffic of POA (left panel) and VOC (right panel) in tonnes per year.

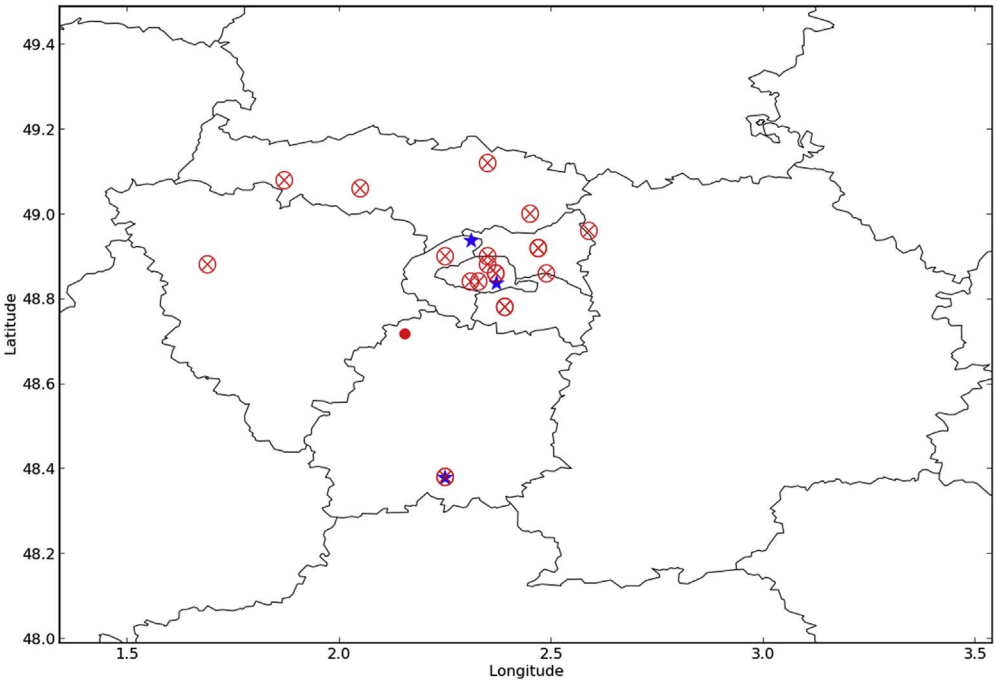

Fig. 5. Measurement sites at which simulated concentrations are compared (PM_{10} and $PM_{2.5}$ sites are represented with red big dots, BC sites are represented with blue stars and the OA site is represented with a red bullet. (For interpretation of the references to colour in this figure legend, the reader is referred to the Web version of this article.)

Table 1
Statistics of comparisons to measurements for O_3 and NO_2. The statistics are derived from hourly concentrations for a year.

	Number of stations	Meas. mean	Sim. mean	Correlation	mfe	mfb
		($\mu g\,m^{-3}$)	($\mu g\,m^{-3}$)	(%)	(%)	(%)
O_3	23	47.5	72.3	64	15.1	4.2
NO_2	18	26.8	18.6	57	49.9	−24.6

Table 2
Statistics of comparisons to measurements for PM_{10}, $PM_{2.5}$, BC and OA. The statistics are derived from daily concentrations for a year.

	Number of stations	Meas. mean	Sim. mean	Correlation	mfe	mfb
		($\mu g\,m^{-3}$)	($\mu g\,m^{-3}$)	(%)	(%)	(%)
PM_{10}	14	21.1	17.3	32	43.6	−23.8
$PM_{2.5}$	7	12.4	14.2	36	45.4	21.6
BC	3	1.2	0.6	75	64.6	−60.9
OA	1	3.2	2.2	41	50.9	−29.8

computed using the POA_{total}/VOC emission ratios rather than the POA_{total}/POA emission ratio. The difference between the reference and the sensitivity simulations is of opposite sign for emissions and concentrations. This is explained by differences in the volatility of POA_{total} emissions estimated from the POA_{total}/POA emission ratio and those estimated from the POA_{total}/VOC emission ratios. POA_{total} emissions calculated from the POA_{total}/VOC emission ratios are distributed into classes of higher volatility than those calculated from the POA_{total}/POA emission ratio. Thus the fraction of OA in the particle phase is lower in the simulation where emissions are calculated from the POA_{total}/VOC emission ratio. Indeed, Fig. 8 shows that the total organic (gas and particle phase OA) concentrations are between 10 and 25% higher in the simulation obtained with emissions estimated from the POA_{total}/VOC emission ratios than in the one with emissions estimated from the POA_{total}/POA emission ratio, in agreement with the observed variations between the emissions of the two simulations (up to between 120% and 140% in Central Paris).

4. Conclusion

High organic aerosol concentrations observed in cities during wintertime result in part from ageing of gas-phase precursors emitted from traffic exhaust. Organic aerosol precursors are emitted in the gas phase, as VOC and/or as compounds of lower volatility (POA_{vapor}).

The policies to reduce emissions of primary particles ($PM_{2.5}$) have been implemented with the introduction of diesel particle filters. Organic secondary concentrations have also been indirectly regulated with efforts in reducing VOC emissions of gasoline vehicles. Simulations over the year 2014 show that VOC do not contribute much to SOA formation over Greater Paris (less than 5%). However, POA_{vapor}, which are not directly regulated, may strongly contribute to SOA formation, especially over Central Paris. Gas and particle phase primary emissions (POA_{total}) are usually estimated in air-quality models from emissions of primary organic aerosols in the particle phase (POA). However, these POA emissions are often not directly available from emission inventories, and they are estimated from particulate matter emissions using a speciation coefficient. Furthermore, they are subject to large uncertainty, as they vary with temperature because of their partitioning between the gas and particle phases.

In this work, a parameterisation based on chamber experiments is used to estimate POA_{total} emissions from VOC emissions for both diesel and gasoline vehicles. POA_{total} emissions are estimated to be larger over urban areas than estimated using primary organic aerosol emissions (up to between 120% and 140% in Central Paris). However, the opposite is observed along motorways axes (between −50% and −70%). Differences between OA_{total} concentrations (gas and particle phases) computed using the two different approaches to estimate POA_{total} emissions and volatilities lead to differences between −8% and 25%, that is lower than differences in emissions (which range between −70% and 140%). The effect on organic aerosol OA concentrations (particle phase) depends strongly on the volatility of the emissions: even though OA_{total} concentrations increase over Central Paris in the sensitivity study here, OA concentrations decrease because of differences in the volatility of emissions.

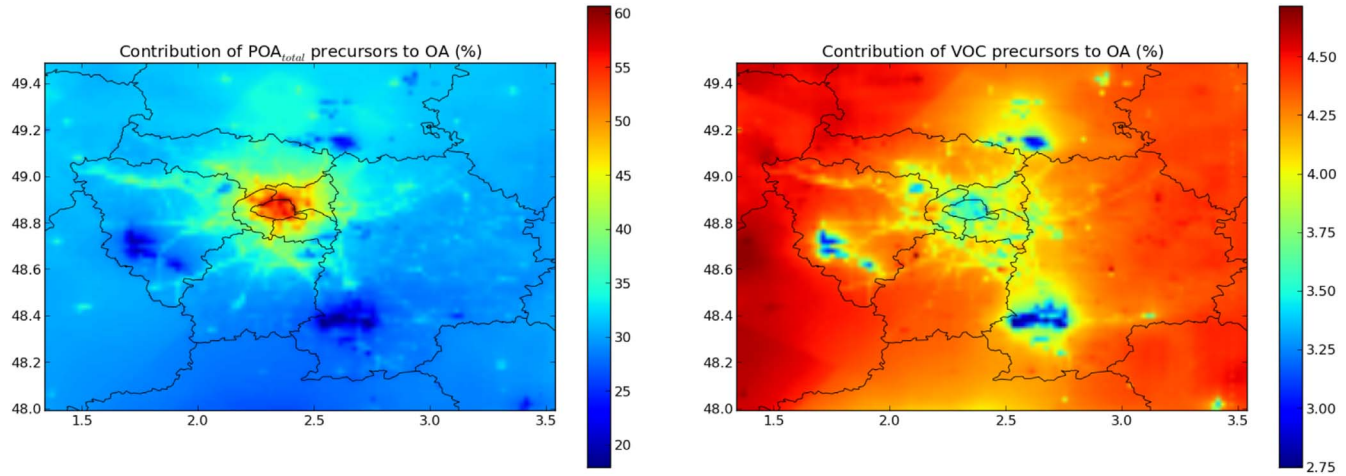

Fig. 6. Contribution in % of POA_{total} emissions (left panel) and VOC emissions (right panel) to OA concentrations.

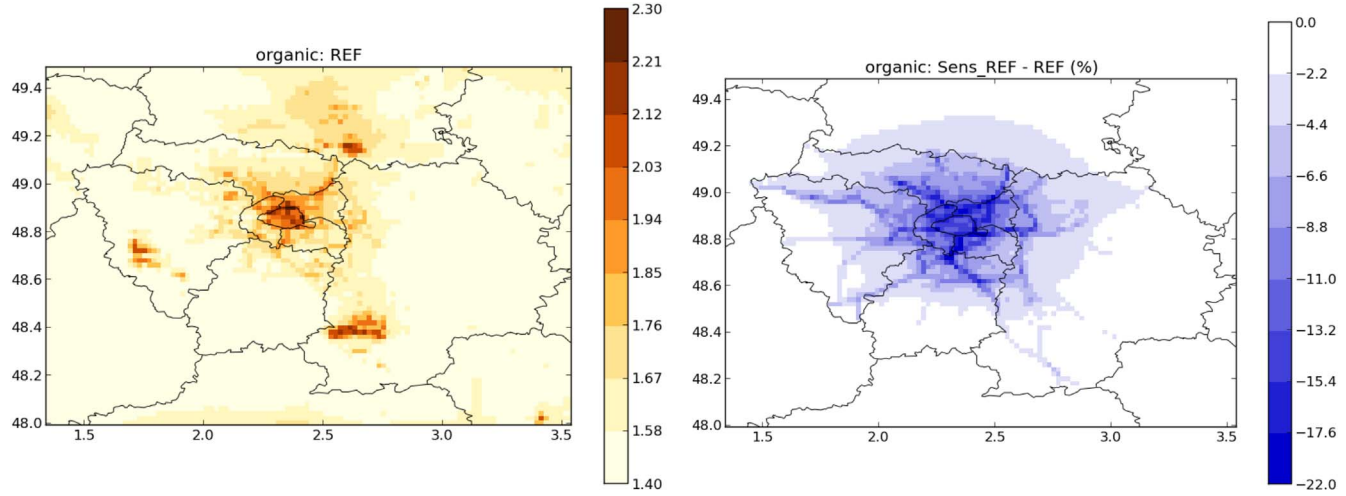

Fig. 7. Organic aerosol concentrations (particle phase OA) in $\mu g\ m^{-3}$ simulated with emissions estimated from the POA_{total}/POA emission ratio (left panel) and relative differences (in %) between concentrations simulated with emissions estimated from the POA_{total}/VOC emission ratios and those simulated with emissions estimated from the POA_{total}/POA emission ratio (right panel).

The parameterisation used here to estimate emissions of intermediate, semi and low volatile organic compounds is based on chamber experiments. However, it is subject to a high level of uncertainties, due in part to the low number of European vehicles on which the parameterisation was tested, but also to uncertainties in the characterization of emissions and their volatilities, and uncertainties in representing

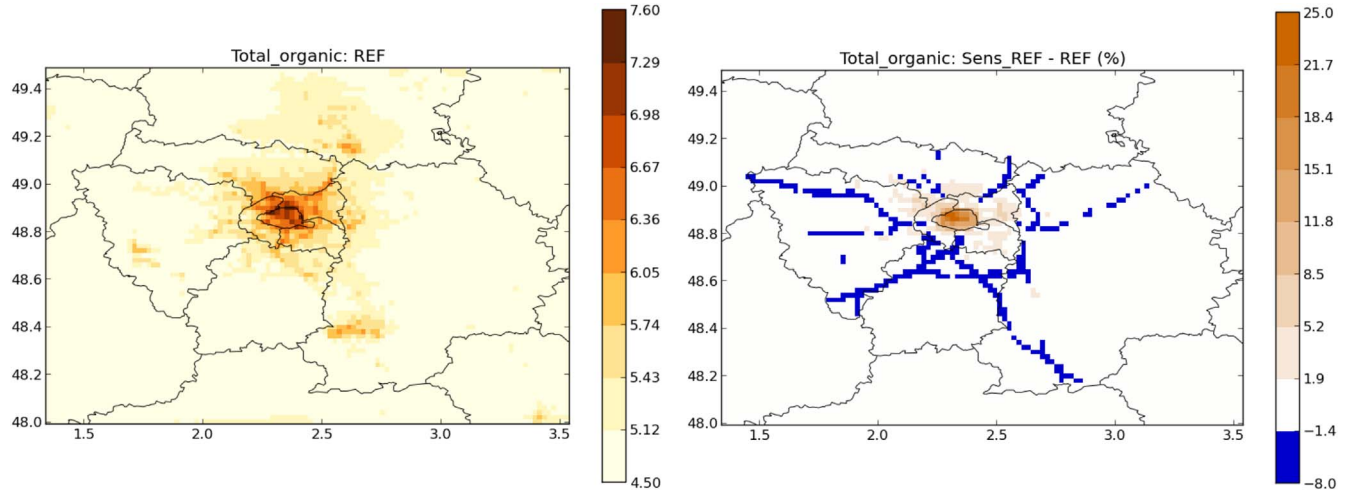

Fig. 8. Total organic concentrations (gas + particle phase OA_{total}) in $\mu g\ m^{-3}$ simulated with emissions estimated from the POA_{total}/POA emission ratio (left panel) and relative differences (in %) between concentrations simulated with emissions estimated from the POA_{total}/VOC emission ratios and those simulated with emissions estimated from the POA_{total}/POA emission ratio (right panel).

chamber wall losses. Regarding organic aerosol concentrations, the air-quality model is validated here against measurements performed at one site in Greater Paris. Other measurement sites, particularly in Central Paris where the impact of intermediate, semi and low volatile organic compound emissions from traffic is high, are required to validate the model extensively.

Acknowledgment

This study received a financial support from the French Agency for Food, Environmental and Occupational Health & Safety (Anses) through Grant 2016-CRD-04 and is part of the work initiated by the Anses working group on ambient particulate matter (chemical composition and road traffic emissions) whose members are André M., André J.M., Baeza-Squiban A., Blanchard M., Charron A., Gagnepain L., Garçon G., Honoré C. (from May to December 2016), Jacquemin B., Moukhtar S., Mullot J.U. and Sartelet K. The analyses, interpretations and conclusions in the present study are those of the authors and do not necessarily reflect those of the mentioned institutions. Organic aerosol measurements at SIRTA have been performed in the frame of the EU ACTRIS program and supported at the national level by the CLAP initiative.

Appendix A. Glossary

Table A.3
Notations used in this paper, following the naming convention of Murphy et al. (2014).

OA	Particle phase organic aerosol concentration
OA_{vapor}	Gas phase organic aerosol concentration
OA_{total}	Gas and particle phase organic aerosol concentration
POA	Primary particle phase organic aerosol
POA_{vapor}	Primary gas phase organic aerosol
POA_{total}	Primary gas and particle phase organic aerosol
POA-iv	Primary (gas and particle phase) organic aerosol of intermediate volatility
POA-sv	Primary (gas and particle phase) organic aerosol of semi volatility
POA-lv	Primary (gas and particle phase) organic aerosol of low volatility
SOA	Secondary particle phase organic aerosol
SOA_{vapor}	Secondary gas phase organic aerosol
SOA-iv	Secondary (gas and particle phase) organic aerosol of intermediate volatility
SOA-sv	Secondary (gas and particle phase) organic aerosol of semi volatility
SOA-lv	Secondary (gas and particle phase) organic aerosol of low volatility
VOC	Volatile organic compounds
NMHC	Non methane hydrocarbons

Appendix B. Distribution of POA_{total} emissions in volatility classes

Table B.4
Distribution of POA_{total} emissions of diesel vehicles without DPF in volatility classes (classified by their saturation concentration c^*), as measured by Zhao et al. (2015), and as modelled here.

log(c^*)	Fraction of POA_{total}	Model species	Model log(c^*)	Model fraction of POA_{total}
< -1	0.034	POA-lv	−0.04	0.041
−1	0.007			
0	0.008			
1	0.025	POA-sv	1.93	0.058
2	0.025			
3	0.079			
4	0.203	POA-iv	3.5	0.612
5	0.330			
6	0.289			

Table B.5
Distribution of POA_{total} emissions of gasoline vehicles in volatility classes (classified by their saturation concentration c*), as measured by Zhao et al. (2016), and as modelled here.

log(c*)	Fraction of POA_{total}	Model species	Model log(c*)	Model fraction of POA_{total}
< -1	0.026	POA-lv	−0.04	0.031
−1	0.005			

0	0.018			
1	0.098	POA-sv	1.93	0.184
2	0.068			
3	0.057			
4	0.059	POA-iv	3.5	0.247
5	0.131			
6	0.5			

Table B.6
Distribution of POA_{total} emissions of diesel vehicles with DPF in volatility classes (classified by their saturation concentration c*), as measured by Zhao et al. (2015)), and as modelled here.

log(c*)	Fraction of POA_{total}	Model species	Model log(c*)	Model fraction of POA_{total}
< -1	0.024	POA-lv	−0.04	0.026
−1	0.002			
0	0.114			
1	0.058	POA-sv	1.93	0.23
2	0.058			
3	0.068			
4	0.180	POA-iv	3.5	0.529
5	0.281			
6	0.214			

Appendix C. Emissions of modelled POA_{total}

For diesel vehicles:

$$POA\text{-}iv = 0.6\ VOC * 0.612/(0.612 + 0.289) = 0.407\ VOC \quad (C.1)$$

$$POA\text{-}sv = POA\text{-}iv * 0.058/0.612 = POA\text{-}iv * 0.09477 \quad (C.2)$$

$$POA\text{-}lv = POA\text{-}iv * 0.041/0.612 = POA\text{-}iv * 0.067 \quad (C.3)$$

For diesel vehicles with DPF:

$$POA\text{-}iv = 1.5\ VOC * 0.529/(0.529 + 0.214) = 1.068\ VOC \quad (C.4)$$

$$POA\text{-}sv = 0.026/0.529\ POA\text{-}iv = 0.0491\ POA\text{-}iv \quad (C.5)$$

$$POA\text{-}lv = 0.23/0.529\ POA\text{-}iv = 0.435\ POA\text{-}iv \quad (C.6)$$

For hot-start gasoline vehicles:

$$POA\text{-}iv = 0.17 * VOC * 0.247/(0.247 + 0.5) = 0.0562 * VOC \quad (C.7)$$

$$POA\text{-}sv = 0.745 * POA\text{-}iv \quad (C.8)$$

$$POA\text{-}lv = 0.1255 * POA\text{-}iv \quad (C.9)$$

For cold-start gasoline vehicles:

$$POA\text{-}iv = 0.04\ VOC * 0.247/(0.247 + 0.5) = 0.0132\ VOC \quad (C.10)$$

$$POA\text{-}sv = POA\text{-}iv * 0.184/0.247 = POA\text{-}iv * 0.745 \quad (C.11)$$

$$POA\text{-}lv = POA\text{-}iv * 0.031/0.247 = POA\text{-}iv * 0.1255 \quad (C.12)$$

References

Baudic, A., Gros, V., Sauvage, S., Locoge, N., Sanchez, O., Sarda-Estève, R., Kalogridis, C., Petit, J.E., Bonnaire, N., Baisnée, D., Favez, O., Albinet, A., Sciare, J., Bonsang, B., 2016. Seasonal variability and source apportionment of volatile organic compounds (VOCs) in the Paris megacity (France). Atmos. Chem. Phys. 16, 11961–11989.

Beekmann, M., Prévôt, A., Drewnick, F., Sciare, J., Pandis, S., Denier van der Gon, H., Crippa, M., Freutel, F., Poulain, L., Ghersi, V., Rodriguez, E., Beirle, S., Zotter, P., von der Weiden-Reinmüller, S.L., Bressi, M., Fountoukis, C., Petetin, H., Szidat, S., Schneider, J., Rosso, A., El Haddad, I., Megaritis, A., Zhang, Q., Michoud, V., Slowik, J., Moukhtar, S., Kolmonen, P., Stohl, A., Eckhardt, S., Borbon, A., Gros, V., Marchand, N., Jaffrezo, J., Schwarzenboeck, A., Colomb, A., Wiedensohler, A., Borrmann, S., Lawrence, M., Baklanov, A., Baltensperger, U., 2015. In situ, satellite measurement and model evidence on the dominant regional contribution to fine particulate matter levels in the Paris megacity. Atmos. Chem. Phys. 15, 9577–9591.

Bergström, R., Denier van der Gon, H., Prévôt, A., Yttri, K., Simpson, D., 2012. Modelling of organic aerosols over Europe (2002-2007) using a volatility basis set (VBS) framework: application of different assumptions regarding the formation of secondary

organic aerosol. Atmos. Chem. Phys. 12, 8499–8527.
Boylan, J., Russell, A., 2006. PM and light extinction model performance metrics, goals, and criteria for three-dimensional air quality models. Atmos. Environ. 40, 4946–4959.
Cheng, Z., Luo, L., Wang, S., Wang, Y., Sharma, S., Shimadera, H., Wang, X., Bressi, M., de Miranda, R., Jiang, J., Zhou, W., Fajardo, O., Yan, N., Hao, J., 2016. Status and characteristics of ambient $PM_{2.5}$ pollution in global megacities. Environ. Int. 89, 212–221.
Chrit, M., Sartelet, K., Sciare, J., Pey, J., Marchand, N., Couvidat, F., Sellegri, K., Beekmann, M., 2017. Modelling organic aerosol concentrations and properties during ChArMEx summer campaigns of 2012 and 2013 in the western Mediterranean region. Atmos. Chem. Phys. 17, 12509–12531.
Couvidat, F., Sartelet, K., 2015. The Secondary Organic Aerosol Processor (SOAP) model: a unified model with different ranges of complexity based on the molecular surrogate approach. Geosci. Model Dev. 8, 1111–1138.
Couvidat, F., Debry, É., Sartelet, K., Seigneur, C., 2012. A hydrophilic/hydrophobic organic (H^2O) aerosol model: development, evaluation and sensitivity analysis. J. Geophys. Res. 117.
Couvidat, F., Kim, Y., Sartelet, K., Seigneur, C., Marchand, N., Sciare, J., 2013. Modeling secondary organic aerosol in an urban area: application to Paris, France. Atmos. Chem. Phys. 13, 983–996.
Dawson, M., Xu, J., Griffin, R., Dabdub, D., 2016. Development of aroCACM/MPMPO 1.0: a model to simulate secondary organic aerosol from aromatic precursors in regional models. Geosci. Model Dev. 9, 2143–2151.
Denier van der Gon, H.A.C., Bergström, R., Fountoukis, C., Johansson, C., Pandis, S., Simpson, D., Visschedijk, A., 2015. Particulate emissions from residential wood combustion in Europe: revised estimates and an evaluation. Atmos. Chem. Phys. 15, 6503–6519.
Dunmore, R., Hopkins, J., Lidster, R., Lee, J., Evans, M., Rickard, A., Lewis, A., Hamilton, J., 2015. Diesel-related hydrocarbons can dominate gas phase reactive carbon in megacities. Atmos. Chem. Phys. 15, 9983–9996.
Dzepina, K., Volkamer, R., Madronich, S., Tulet, P., Ulbrich, I., Zhang, Q., Cappa, C., Ziemann, P., Jimenez, J., 2009. Evaluation of recently-proposed secondary organic aerosol models for a case study in Mexico City. Atmos. Chem. Phys. 9, 5681–5709.
Emmons, L.K., Walters, S., Hess, P.G., Lamarque, J.F., Pfister, G.G., Fillmore, D., Granier, C., Guenther, A., Kinnison, D., Laepple, T., Orlando, J., Tie, X., Tyndall, G., Wiedinmyer, C., Baughcum, S.L., Kloster, S., 2010. Description and evaluation of the model for ozone and related chemical tracers, version 4 (MOZART-4). Geosci. Model Dev. 3, 43–67.
Gentner, D., Jathar, S., Gordon, T., Bahreini, R., Day, D., El Haddad, I., Hayes, P., Pieber, S., Platt, S., de Gouw, J., Goldstein, A., Harley, R., Jimenez, J., Prévôt, A., Robinson, A., 2017. Review of urban secondary organic aerosol formation from gasoline and diesel motor vehicle emissions. Environ. Sci. Technol. 51, 1074–1093.
Gierczak, C., Kralik, L., Mauti, A., Harwell, A., Maricq, M., 2017. Measuring NMHC and NMOG emissions from motor vehicles via FTIR spectroscopy. Atmos. Environ. 150, 425–433.
Gordon, T., Presto, A., May, A., Nguyen, N., Lipsky, E., Donahue, N., Gutierrez, A., Zhang, M., Maddox, C., Rieger, P., Chattopadhyay, S., Maldonado, H., Maricq, M., Robinson, A., 2014a. Secondary organic aerosol formation exceeds primary particulate matter emissions for light-duty gasoline vehicles. Atmos. Chem. Phys. 14, 4661–4678.
Gordon, T., Presto, A., Nguyen, N., Robertson, W., Na, K., Sahay, K., Zhang, M., Maddox, C., Rieger, P., Chattopadhyay, S., Maldonado, H., Maricq, M., Robinson, A., 2014b. Secondary organic aerosol production from diesel vehicle exhaust: impact of aftertreatment, fuel chemistry and driving cycle. Atmos. Chem. Phys. 14, 4643–4659.
Guenther, A., Karl, T., Harley, P., Wiedinmyer, C., Palmer, P., Geron, C., 2006. Estimates of global terrestrial isoprene emissions using MEGAN (model of emissions of gases and aerosols from nature). Atmos. Chem. Phys. 6, 3181–3210.
Hayes, P., Carlton, A., Baker, K., Ahmadov, R., Washenfelder, R., Alvarez, S., Rappenglück, B., Gilman, J., Kuster, W., de Gouw, J., Zotter, P., Prévôt, A., Szidat, S., Kleindienst, T., Offenberg, J., Ma, P., Jimenez, J., 2015. Modeling the formation and aging of secondary organic aerosols in Los Angeles during CalNex 2010. Atmos. Chem. Phys. 15, 5773–5801.
Hodzic, A., Jimenez, J., Madronich, S., Canagaratna, M., DeCarlo, P., Kleinman, L., Fast, J., 2010. Modeling organic aerosols in a megacity: potential contribution of semi-volatile and intermediate volatility primary organic compounds to secondary organic aerosol formation. Atmos. Chem. Phys. 10, 5491–5514.
Jaeglé, L., Quinn, P.K., Bates, T.S., Alexander, B., Lin, J.T., 2011. Global distribution of sea salt aerosols: new constraints from in situ and remote sensing observations. Atmos. Chem. Phys. 11, 3137–3157.
Jathar, S., Donahue, N., Adams, P., Robinson, A., 2014a. Testing secondary organic aerosol models using smog chamber data for complex precursor mixtures: influence of precursor volatility and molecular structure. Atmos. Chem. Phys. 14, 5771–5780.
Jathar, S., Gordon, T., Hennigan, C., Pye, H., Pouliot, G., Adams, P., Donahue, N., Robinson, A., 2014b. Unspeciated organic emissions from combustion sources and their influence on the secondary organic aerosol budget in the United States. Proc. Natl. Acad. Sci. Unit. States Am. 111, 10473–10478.
Jathar, S., Woody, M., Pye, H., Baker, K., Robinson, A., 2017. Chemical transport model simulations of organic aerosol in southern California: model evaluation and gasoline and diesel source contributions. Atmos. Chem. Phys. 17, 4305–4318.
Jimenez, J., Canagaratna, M., Donahue, N., Prevot, A., Zhang, Q., Kroll, J., DeCarlo, P., Allan, J., Coe, H., Ng, N., Aiken, A., Docherty, K., Ulbrich, I., Grieshop, A., Robinson, A., Duplissy, J., JD, S., KR, W., VA, L., Hueglin, C., Sun, Y., Tian, J., Laaksonen, A., Raatikainen, T., Rautiainen, J., Vaattovaara, P., Ehn, M., Kulmala, M., Tomlinson, J., Collins, D., Cubison, M., Dunlea, E., Huffman, J., Onasch, T., Alfarra, M., Williams, P., Bower, K., Kondo, Y., Schneider, J., Drewnick, F., Borrmann, S., Weimer, S., Demerjian, K., Salcedo, D., Cottrell, L., Griffin, R., Takami, A., Miyoshi, T., Hatakeyama, S., Shimono, A., Sun, J., Zhang, Y., Dzepina, K., Kimme, J., Sueper, D., Jayne, J., Herndon, S., Trimborn, A., Williams, L., Wood, E., Middlebrook, A., Kolb, C., Baltensperger, U., Worsnop, D., 2009. Evolution of organic aerosols in the atmosphere. Science 326, 1525–1529.
Kim, Y., Couvidat, F., Sartelet, K., Seigneur, C., 2011. Comparison of different gas-phase mechanisms and aerosol modules for simulating particulate matter formation. J. Air Waste Manag. Assoc. 61, 1218–1226.
Kim, Y., Sartelet, K., Raut, J., Chazette, P., 2013. Evaluation of the weather research and forecast/urban model over greater Paris. Boundary-Layer Meteorol. 149, 105–132.
Kim, Y., Sartelet, K., Seigneur, C., Charron, A., Besombes, J.L., Jaffrezo, J.L., Marchand, N., Polo, L., 2016. Effect of measurement protocol on organic aerosol measurements of exhaust emissions from gasoline and diesel vehicles. Atmos. Environ. 140, 176–187.
Koo, B., Knipping, E., Yarwood, G., 2014. 1.5- Dimensional volatility basis set approach for modeling organic aerosol in CAMx and CMAQ. Atmos. Environ. 95, 158–164.
Kuwayama, T., Collier, S., Forestieri, S., Brady, J., Bertram, T., Cappa, C., Zhang, Q., Kleeman, M., 2015. Volatility of primary organic aerosol emitted from light duty gasoline vehicles. Environ. Sci. Technol. 49, 1569–1577.
Louis, C., Liu, Y., Tassel, P., Perret, P., Chaumond, A., André, M., 2016. PAH, BTEX, carbonyl compound, black-carbon, NO_2 and ultrafine particle dynamometer bench emissions for Euro 4 and Euro 5 diesel and gasoline passenger cars. Atmos. Environ. 141, 80–95.
Martinet, S., Liu, Y., Louis, C., Tassel, P., Perret, P., Chaumond, A., André, M., 2017. Euro 6 unregulated pollutant characterization and statistical analysis of after-treatment device and driving-condition impact on recent passenger-car emissions. Environ. Sci. Technol. 51, 5847–5855.
May, A., Presto, A., Hennigan, C., Nguyen, N., Gordon, T., Robinson, A., 2013a. Gas-particle partitioning of primary organic aerosol emissions: (1) Gasoline vehicle exhaust. Atmos. Environ. 77, 128–139.
May, A., Presto, A., Hennigan, C., Nguyen, N., Gordon, T., Robinson, A., 2013b. Gas-particle partitioning of primary organic aerosol emissions: (2) diesel vehicles. Environ. Sci. Technol. 47, 8288–8296.
May, A., Nguyen, N., Presto, A., Gordon, T., Lipsky, E., Karve, M., Gutierre, A., Robertso, W., Zhang, M., Brandow, C., Chang, O., Chen, S., Cicero-Fernandez, P., Dinkins, L., Fuentes, M., Huang, S.M., Ling, R., Long, J., Maddox, C., Massetti, J., McCauley, E., Miguel, A., Na, K., Ong, R., Pang, Y., Rieger, P., Sax, T., Truong, T., Vo, T., Chattopadhyay, S., Maldonado, H., Maricq, M., Robinson, A., 2014. Gas- and particle-phase primary emissions from in-use, on-road gasoline and diesel vehicles. Atmos. Environ. 88, 247–260.
Murphy, B., Donahue, N., Robinson, A., Pandis, S., 2014. A naming convention for atmospheric organic aerosol. Atmos. Chem. Phys. 14, 5825–5839.
Murphy, B., Woody, M., Jimenez, J., Carlton, A., Hayes, P., Liu, S., Ng, N., Russell, L., Setyan, A., Xu, L., Young, J., Zaveri, R., Zhang, Q., Pye, H., 2017. Semivolatile POA and parameterized total combustion SOA in CMAQv5.2: impacts on source strength and partitioning. Atmos. Chem. Phys. 17, 11107–11133.
Ntziachristos, L., Samaras, Z., Kouridis, C., Hassel, D., Mellios, G., McCrae, I., Hickman, J., Zierock, K.H., Keller, M., Rexeis, M., Andre, M., Winther, M., Pastramas, N., Gorissen, N., Boulter, P., Katsis, P., Joumard, R., Rijkeboer, R., Geivanidis, S., Hausberger, S., 2008. Exhaust Emissions from Road Transport, EMEP Guidebook 2014.
Ntziachristos, L., Papadimitriou, G., Ligterink, N., Hausberger, S., 2016. Implications of diesel emissions control failures to emission factors and road transport NOx evolution. Atmos. Environ. 141, 542–551.
Odum, J., Jungkamp, T., Griffin, R., Flagan, R., Seinfeld, J., 1997. The atmospheric aerosol-forming potential of whole gasoline vapor. Science 276, 96–99.
Ots, R., Young, D., Vieno, M., Xu, L., Dunmore, R., Allan, J., Coe, H., Williams, L., Herndon, S., Ng, N., Hamilton, J., Begström, R., Di Marco, C., Nemitz, E., Mackenzie, I., Kuenen, J., Green, D., Reis, S., Heal, M., 2016. Simulating secondary organic aerosol from missing diesel-related intermediate-volatility organic compound emissions during the Clean Air for London (ClearfLo) campaign. Atmos. Chem. Phys. 16, 6453–6473.
Petit, J.E., Favez, O., Sciare, J., Crenn, V., Sarda-Estève, R., Bonnaire, N., Močnik, G., Dupont, J.C., Haeffelin, M., Leoz-Garziandia, E., 2015. Two years of near real-time chemical composition of submicron aerosols in the region of Paris using an Aerosol Chemical Speciation Monitor (ACSM) and a multi-wavelength Aethalometer. Atmos. Chem. Phys. 15, 2985–3005.
Platt, S., El Haddad, I., Zardini, A., Clairotte, M., Astorga, C., Wolf, R., Slowik, J., Temime-Roussel, B., Marchand, N., Jezek, I., Drinovec, L., Mocnik, G., Möhler, O., Richter, R., Barmet, P., Bianchi, F., Baltensperger, U., Prévôt, S., 2013. Secondary organic aerosol formation from gasoline vehicle emissions in a new mobile environmental reaction chamber. Atmos. Chem. Phys. 13, 9141–9158.
Pope, C., Thun, M., Namboodiri, M., Dockery, D., Evans, J., Speizer, F., Heath, C., 1995. Particulate air pollution as a predictor of mortality in a prospective study of U.S. adults. Am. J. Respir. Crit. Care Med. 151, 669–674.
Robinson, A., Donahue, N., Shrivastava, M., Weitkamp, E., Sage, A., Grieshop, A., Lane, T., Pierce, J., Pandis, S., 2007. Rethinking organic aerosols: semivolatile emissions and photochemical aging. Science 315, 1259–1262.
Roustan, Y., Pausader, M., Seigneur, C., 2011. Estimating the effect of on-road vehicle emission controls on future air quality in Paris, France. Atmos. Environ. 45, 6828–6836.
Russell, A., Dennis, R., 2000. NARSTO critical review of photochemical models and modeling. Atmos. Environ. 34 2,283–2,234.
Sartelet, K., Couvidat, F., Seigneur, C., Roustan, Y., 2012. Impact of biogenic emissions on air quality over Europe and North America. Atmos. Environ. 53, 131–141.
Schauer, J.J., Kleeman, M., Cass, G., Simoneit, B., 1999. Measurement of emissions from air pollution sources. 2. C1 through C30 organic compounds from medium duty diesel trucks. Environ. Sci. Technol. 33, 1578–1587.

Schauer, J.J., Kleeman, M., Cass, G., Simoneit, B., 2002. Measurement of emissions from air pollution sources. 5. C1-C32 organic compounds from gasoline-powered motor vehicles. Environ. Sci. Technol. 36, 1169–1180.

Skamarock, W., Klemp, J., Dudhia, J., Gill, D., Barker, D., Duda, M., Huang, X., Wang, W., Powers, J., 2008. A Description of the Advanced Research WRF. NCAR Technical Note, NCAR/TN\ u2013475? STR. pp. 123. version 3.

Terrenoire, E., Bessagnet, B., Roul, L., Tognet, F., Pirovano, G., Létinois, L., Beauchamp, M., Colette, A., Thunis, P., Amann, M., Menut, L., 2015. High-resolution air quality simulation over Europe with the chemistry transport model CHIMERE. Geosci. Model Dev. 8, 21–42.

Theloke, J., Friedrich, R., 2007. Compilation of database on the composition of anthropogenic VOC emissions for atmospheric modeling in Europe. Atmos. Environ. 41, 4148–4160.

Vestreng, V., 2003. Review and Revision: Emission Data Reported to CLRTAP, EMEP/MSC-w Note 1/2003. Norw. Meteorol. Inst., Oslo.

Woody, M., Baker, K., Hayes, P., Jimenez, J., Koo, B., Pye, H., 2016. Understanding sources of organic aerosol during CalNex-2010 using the CMAQ-VBS. Atmos. Chem. Phys. 16, 4081–4100.

Zhang, Q., Jimenez, J., Canagaratna, M., Allan, J., Coe, H., Ulbrich, I., Alfarra, M., Takami, A., Middlebrook, A., Sun, Y., Dzepina, K., Dunlea, E., Docherty, K., DeCarlo, P., Salcedo, D., Onasch, T., Jayne, J., Miyoshi, T., Shimono, A., Hatakeyama, S., Takegawa, N., Kondo, Y., Schneider, J., Drewnick, F., Borrmann, S., Weimer, S., Demerjian, K., Williams, P., Bower, K., Bahreini, R., Cottrell, L., Griffin, R., Rautiainen, J., Sun, J., Zhang, Y., Worsnop, D., 2007. Ubiquity and dominance of oxygenated species in organic aerosols in anthropogenically-influenced Northern Hemisphere midlatitudes. Geophys. Res. Lett. 34, L13801.

Zhang, Y., Sartelet, K., Zhu, S., Wang, W., Wu, S.Y., Zhang, X., Wang, K., Tran, P., Seigneur, C., Wang, Z.F., 2013. Application of WRF/Chem-MADRID and WRF/Polyphemus in Europe - Part 2: evaluation of chemical concentrations, sensitivity simulations, and aerosol-meteorology interactions. Atmos. Chem. Phys. 13, 6845–6875.

Zhao, Y., Nguyen, N., Presto, A., Hennigan, C., May, A., Robinson, A., 2015. Intermediate volatility organic compound emissions from on-road diesel vehicles: chemical composition, emission factors, and estimated secondary organic aerosol production. Environ. Sci. Technol. 49, 11516–11526.

Zhao, Y., Nguyen, N., Presto, A., Hennigan, C., May, A., Robinson, A., 2016. Intermediate volatility organic compound emissions from on-road gasoline vehicles and small off-road gasoline engines. Environ. Sci. Technol. 50, 4554–4563.

Zhu, S., Sartelet, K., Healy, R., Wenger, J., 2016. Simulation of particle diversity and mixing state over Greater Paris: a model-measurement inter-comparison. Faraday Discuss 189, 547–566.